Supplemental Material for Chavez et al., Homologous recombination-dependent rescue of deficiency in the structural maintenance of chromosomes (Smc) 5/6 complex

METHODS:

Yeast co-immunoprecipitation:

50 ml of exponentially growing yeast cells were harvested and washed in ice-cold water, and all further steps were at 4^0C. Cells were resuspended in 600 µl lysis buffer (50 mM Tris-Cl pH 8, 5% glycerol, 125 mM KCl, 0.1% Nonidet P-40, 0.1 mM DTT, $1/7^{th}$ volume of complete protease inhibitors (Roche), 1 mM PMSF, 1 µg/ml each of pepstatin A, leupeptin and aprotinin, 5 mM NaF) and 700 µl of glass beads were also added. Cells were lysed with 3 x 30 second bursts using a bead-beater (Stratech) removing cells to ice between bursts. Extracts were then collected and spun at 14K RPM in a microfuge for 10 minutes to clear the extract. Protein concentrations were determined by Bradford assay.

Each co-IP used 550 µg of protein in a volume of 150 µl, which was precleared *via* rotation for five minutes with 15 µl of Protein G agarose beads (prewashed in lysis buffer) followed by microcentrifugation for 1 minute at 14K RPM. At this point 15 µl of the pre-cleared extract was saved as "input" and placed on ice for the remainder of the experiment, and 135 µl was carried forward for the co-IP. An additional 55 µl of lysis buffer was added along with 10 µl of 50% bead slurry containing 5 µg of pre-bound goat-anti-Myc tag antibody (Abcam #9132) in a 250 µl tube. Binding reactions were rotated for 4 hours, spun (4K RPM in a microfuge), and beads were washed 3x with 200 µl of lysis buffer (including inversion 10x per wash). Beads were suspended in 30 µl of 2x Laemmli sample buffer, heated to 95^0C for 5 minutes followed by a brief spin. The supernatant was electrophoresed on 4-15% gradient gels, and proteins were transferred to nitrocellulose membranes which were probed with anti-YFP (Sigma # G1544) or anti-Myc antibody (Abcam #18185) followed by ECL detection.

Supplemental Table I

Deletions of the following genes were tested in the initial SGA screen, in which *MPH1* deletion was found to suppress the temperature sensitivity of *smc6-9* mutants.

SGS1	*ESC2*	*SLX1*	*TOP1*
NUP60	*YKU70*	*SLX4*	*CTF4*
NUP84	*MAD1*	*MUS81*	*RAD6*
NUP120	*SRS2*	*MMS4*	*RMI1*
NUP133	*RRM3*	*TSA1*	*MRC1*
POL32	*MPH1*	*RAD53*	*RAD27*
SLX5	*SLX8*		

Supplemental Table II Yeast strains and plasmids used in this study

YEAST STRAINS:

All strains are derived from the BY4741/4742 background unless otherwise noted.

CGC1428* MATa, *bar1Δ leu2-3,112 ura3-52 his3-Δ200 trp1-Δ63 ade2-1 lys2-801 pep4, smc6-9-3HA::HIS3*

YAC186 MATa, *mms21-sp::URA3, lys2Δ MET15, cir^0*

YAC187 MATα, *mms21-sp::URA3, lys2Δ MET15, cir^0*

YAC306 MATa, *smc6-9-3HA*::*HIS3*

YAC307 MATα, *smc6-9-3HA::HIS3*

Y8205[Φ] MATα, *can1Δ::STE2pr:Sp-his5, lyp1Δ::STE3pr:LEU2, his3Δ1 leu2Δ0 ura3Δ0*

YAC317 MATα, *mms21-sp::URA3*

YAC399 Y8205 *mms21-sp::URA3*

YAC411 Y8205 *smc6-9-3HA::HIS3*

YAC751 MATa, *sgs1Δ::HIS3*

YAC753 MATa, *sgs1Δ::HIS3, mms21-sp::URA3*

YAC779 MATa, *sgs1Δ::HIS3, mph1Δ::KanMX*

YAC781 MATa, *mms21-sp::URA3, mph1Δ::KanMX*

YAC782 MATα, *mms21-sp::URA3, mph1Δ::KanMX*

YAC784 MATa, *smc6-9-3HA::HIS3, mph1Δ::KanMX*

YAC785 MATα, *smc6-9-3HA::HIS3, mph1Δ::KanMX*

YAC779 MATa, *sgs1Δ::HIS3, mph1Δ::KanMX*

YAC815 MATa, *sgs1Δ::LEU2, mms21-sp::URA3*

YAC817 MATa, *sgs1Δ::LEU2, mms21-sp::URA3, mph1Δ::KanMX*

YAC823 MATa, *smc6-9-3HA::HIS3, sgs1Δ::LEU2, mph1Δ::KanMX*

YAC826 MATα, *mms21-sp::URA3, rad52Δ::HygB*

YAC827 MATα, *mms21-sp::URA3, rad52Δ::HygB, mph1Δ::KanMX*

YAC829 MATα, *smc6-9-3HA::HIS3, rad52Δ::HygB*

YAC830 MATα, *smc6-9-3HA::HIS3, rad52Δ::HygB, mph1Δ::KanMX*

985-7c[π] MATa, *mcd1-1, trp1-1, ura3-52, bar1, gal*

K6013[ψ] MATa, *smc1-259, ade2-1, trp1-1, can1-100, leu2-3,112, his3-11,15*

YAC936 MATa, *mph1Δ::HygB*

YAC938 YAC399, *mph1Δ::HygB*

YAC942 YAC399, *rad53Δ::HygB, sml1Δ::KanMX*

YAC947 YAC411, *rad53Δ::HygB, sml1Δ::KanMX*

YAC963 YAC399, *rad52Δ::KanMX*

YAC965 YAC411, *rad52Δ::KanMX*

YAC1034 MATa, *mph1Δ::NatMX*

YAC1162[€] *smc1-259, mph1Δ::CaURA3, leu2Δ*

YAC1163[€] *mcd1-1, mph1Δ::CaURA3, leu2Δ*

YAC1187 YAC411, *rad5Δ::KanMX*

YAC1133 YAC943, *rad5Δ::KanMX*

YAC1179 YAC411, *rad18Δ::KanMX*

YAC1180 YAC943, *rad18Δ::KanMX*

YAC1181 YAC411, *rad2Δ::KanMX*

YAC1182 YAC943, *rad2Δ::KanMX*

YAC1183 YAC411, *yku70Δ::KanMX*

YAC1184 YAC943, *yku70Δ::KanMX*

YAC1185 YAC411, *rad10Δ::KanMX*

YAC1186 YAC943, *rad10Δ:: KanMX*

PJ69-4a^ MATa, *trp1-901 leu2-3,112 ura3-52 his3-200 gal4Δ gal80Δ LYS2::GAL1-HIS3 GAL2-ADE2 met2::GAL7-lacZ*

PJ69-4α^ MATα, *trp1-901 leu2-3,112 ura3-52 his3-200 gal4Δ gal80Δ LYS2::GAL1-HIS3 GAL2-ADE2 met2::GAL7-lacZ*

PLASMIDS:

For the generation of *SGS1* and *MPH1* expression vectors, pAG413GPD-ccdB, pAG415GPD-ccdB, pAG416GPD-ccdB, pAG416GPD-ccdB-YFP destination vectors (courtesy of Aaron Gitler[&]) were restriction digested with SacI and SpeI to remove the GPD promoter. A PCR fragment containing the region 1kb upstream of either the *SGS1* ORF or *MPH1* ORF and flanked by 5' SacI and 3' SpeI restriction sites was inserted in place of the previous GPD fragment. This created the *SGS1* and *MPH1* CEN/ARS series destination vectors that were used in all subsequent experiments. In the case of the *NOP1* promoter the region 400 bp upstream of the *NOP1* ORF was utilized and incorporated into the pAG vector series in a fashion similar to the *SGS1* and *MPH1* promoters. We have kept with the *S. cerevisiae* Advanced Gateway Destination Vector nomenclature when describing our generated vectors[&]. All entry vectors contain the full length ORF, except where noted.

pAG413GPD-ccdB[&]

pAG415GPD-ccdB[&]

pAG416GPD-ccdB[&]

AC394 pAG415SGS1-ccdB

AC395 pAG416SGS1-ccdB

AC430 pAG413MPH1-ccdB

AC431 pAG415MPH1-ccdB

AC432 pAG416MPH1-ccdB

AC640 pAG413SGS1-ccdB

AC992 pAG413MPH1-TAP-ccdb

AC994 pAG413SGS1-TAP-ccdb

AC504 pDONR221-*MPH1*

AC412 pDONR221-*SGS1*

AC581 pDONR221-*mph1*-D209N-E210Q

AC655 pDONR221-*sgs1-hd* (PCR amplified from vector pJL37[#])

AC656 pDONR221-*sgs1*-Δ*C202* (PCR amplified from vector pJM502[#])

* *Torres-Rosell J, Machin F, Farmer S, Jarmuz A, Eydmann T, Dalgaard JZ, Aragon L (2005) SMC5 and SMC6 genes are required for the segregation of repetitive chromosome regions. Nat Cell Biol 7(4): 412-419*

Φ *Tong AHY, Boone C, Ian S, Michael JRS (2007) 16 High-Throughput Strain Construction and Systematic Synthetic Lethal Screening in. In Methods in Microbiology Vol. Volume 36, pp 369-386, 706-707. Academic Press*

ζ *James P, Halladay J, Craig EA. (1996) Genomic libraries and a host strain designed for highly efficient two- hybrid selection in yeast. Genetics 144: 1425-1436*

π *Guacci V, Koshland D, Strunnikov A (1997) A Direct Link between Sister Chromatid Cohesion and Chromosome Condensation Revealed through the Analysis of MCD1 in S. cerevisiae. Cell 91:47-57*

ψ *Michaelis C, Ciosk R, Nasmyth K (1997) Cohesins: Chromosomal Proteins that Prevent Premature Separation of Sister Chromatids. Cell 91:35-45*

€ *Indicates a haploid derived from a mixed background between BY4742 and the parental strain containing the utilized smc1/3 mutation [K6013 or 985-7c].*

& *Alberti, S., Gitler, A.D. and Lindquist, S. (2007) A suite of Gateway cloning vectors for high-throughput genetic analysis in Saccharomyces cerevisiae. Yeast, 24, 913-919.*

Lu, J., Mullen, J.R., Brill, S.J., Kleff, S., Romeo, A.M. and Sternglanz, R. (1996) Human homologues of yeast helicase. Nature, 383, 678-679.

^ *James, P., Halladay, J., and Craig, E. A. (1996) Genetics 144, 1425-1436*

SUPPLEMENTAL FIGURE LEGENDS

Supplemental Figure 1. Western blot comparing the protein levels expressed from N-terminally TAP tagged *MPH1* alleles. (A) *mms21-sp mph1*Δ mutants containing either TAP-vector control, TAP-*MPH1 or* TAP-*mph1-DE* containing plasmids were grown into mid-log phase and equal numbers of cells were pelleted and lysed for subsequent protein analysis. Extracts were run on 4-15% gradient gels, transferred to nitrocellulose membranes and probed with anti-TAP antibody (Open Biosystems CAB1001). (B) Ponceau S staining of the same nitrocellulose membrane as in panel A, to indicate equal loading of protein among samples.

Supplemental Figure 2. Deletion of *MPH1* reduces accumulation of recombination intermediates in *smc6-9* mutants. (**A**) Representative time course of two-dimensional gel electrophoresis (2DGE) followed by Southern blots examining replication intermediates near *ARS305* in *smc6-9* and *smc6-9 mph1*Δ mutants. (**B**) Bar graph showing quantification of the ratio of X-shaped molecules to structures running within the replication arc at each time point after release into 0.033% MMS.

Supplemental Figure 3. Sgs1 mutants lack robust rescue of DNA damage sensitivity by *MPH1* deletion. Spot assay comparing the growth rates of *sgs1*Δ and *sgs1*Δ *mph1*Δ mutants on the indicated media.

Supplemental Figure 4. Mph1 amino acids 751-810 contain the Smc5 interaction region. (**A**) Two-hybrid analysis comparing the DBD alone or fused to the N-terminus of Smc5 and their ability to interact with AD alone or AD fused to either full length Mph1 or various Mph1-derived polypeptides. Control selects for the presence of both the DBD and AD containing plasmids, -His media selects for the presence of an interaction between the expressed DBD and AD containing proteins. (**B**) Two-hybrid analysis performed similar to (A), demonstrating that amino acids 751-810 of Mph1 are sufficient for interaction with Smc5. Together with the data shown in Figure 3A-B, these findings indicate that Mph1 residues 751-810 contain sequences necessary and sufficient for binding to Smc5.

Supplemental Figure 5. Alignment of Mph1 orthologs with particular focus on the identified SMC5 interaction domain. (A) Whole protein alignment of various Mph1 orthologs demonstrating the location of the Smc5 interacting domain (*SMCI; orange*) with respect to the evolutionarily conserved DEXDc (*blue*) and HELICc (*green*) domains. (B) Sequence alignment within the mapped Smc5 binding domain of Mph1 orthologs demonstrates a region of conservation. Aligned residues are as follows: *S. cerevisiae* (757-795), *H. sapiens* (1658-1694), *D. rerio* (1298-1332), *X. laevis* (1619-1652). Residues identical among all four species are in *red*, and residues identical within a subset of the species are *gray* or *dark gray*.

Supplemental Figure 6. Western blot comparing the protein levels expressed from N-terminally TAP tagged *MPH1* alleles driven by the *MPH1* promoter. (A) *mph1*Δ mutants containing either TAP-*MPH1 or* TAP-*mph1-*Δ*60* containing plasmids were grown into mid-log phase and equal numbers of cells were pelleted and lysed for subsequent protein analysis. Extracts were run on 4-15% gradient gels, transferred to nitrocellulose membranes and probed with anti-TAP antibody (Open Biosystems CAB1001). (B) Ponceau S staining of the same nitrocellulose membrane as in panel A, to indicate equal loading of protein among samples.

Supplemental Figure 7. Sgs1 is required for deletion of *MPH1* to rescue the DNA damage-sensitivity of *smc5/6* mutants. Spot assay comparing the growth rates of the various mutant

strains. Lower MMS and HU concentrations than in Figure 4A are shown to help accentuate any possible small difference between genotypes.

Supplemental Figure 8. Western blot comparing the protein level of N-terminally TAP tagged *SGS1* alleles. (A) *mms21-sp mph1*Δ *sgs1*Δ mutants containing either TAP-*SGS1*, TAP-*sgs1-hd,* or TAP-*sgs1-*Δ*C202* containing plasmids were grown into mid-log phase and equal numbers of cells were pelleted and lysed for subsequent protein analysis. Extracts were run on 4-15% gradient gels, transferred to nitrocellulose membranes and probed with anti-TAP antibody (Open Biosystems CAB1001). (B) Ponceau S staining of the same nitrocellulose membrane as in panel A, to indicate equal loading of protein among samples.

Supplemental Figure 9. Deletion of *MPH1* reduces accumulation of recombination intermediates in *sgs1*Δ mutants. (**A**) Representative time course of two-dimensional gel electrophoresis (2DGE) followed by Southern blots examining replication intermediates near *ARS305* in *sgs1*Δ and *sgs1*Δ *mph1*Δ mutants. (**B**) Quantification of the ratio of X-shaped molecules to structures running within the replication arc at each time point after release into 0.033% MMS.

Supplemental Figure 10. *mph1*Δ-mediated rescue occurs through a Rad51-dependent repair pathway. Spot assay comparing the growth of *smc6-9 rad51*Δ to *smc6-9 rad51*Δ *mph1*Δ mutants on the indicated media. *smc6-9* and *smc6-9 mph1*Δ mutants are provided as a growth reference.

Supplemental Figure 11. *mph1*Δ-mediated rescue is independent of checkpoint proteins as well as factors required for nucleotide excision repair (NER), non-homologous end joining (NHEJ), and single strand annealing (SSA) repair pathways. Spot assay comparing the growth of various *smc6-9* or *smc6-9 mph1*Δ mutants with deletions in genes important for checkpoint activity (*RAD24, RAD9* and *TEL1*), NER (*RAD10* and *RAD2*), NHEJ (*YKU70*), or SSA (*RAD10*).

Supplemental Figure 12$^{\Omega}$. A model for Mph1-dependent and independent repair of damaged replication forks. (**A**) A replication fork that has stalled due to an alkylated base. Mph1 functions early at the stalled fork to facilitate the initiation of template switch recombination repair (repair pathway ABC). The mechanism through which Mph1 facilitates template switch recombination at this time remains unknown but could be *via* direct action at the stalled replication fork or through a hemicatenane-mediated switch process (not shown). (**B**) After switching templates, replication continues using the complementary newly synthesized strand. Once replicated past the lesion, the invading strand then returns to its parental template *via* an HR-dependent mechanism leaving behind a physical linkage between the sister chromatids that is observed upon 2D gel analysis. The biophysical nature of these recombination intermediates have previously been characterized within *sgs1*Δ and *smc5/6* mutants revealing that the accumulated X-shaped molecules represent hemicatenane-like molecules with multiple interlinks, called Rec-X intermediates (1-3). (**C**) Once formed, the Rec-X intermediate is resolved in a manner dependent upon the Sgs1 and Smc5/6 complexes. In the absence of Mph1, repair proceeds down a PRR- and HR-dependent repair pathway (repair pathway ADEFC). The post-replicative repair machinery regresses the stalled replication fork annealing the complementary newly synthesized strands together (not shown). (**D**) Once the fork is regressed, replication off of the newly synthesize complementary strand occurs. After replication is complete, 5'→3' exonuclease activity exposes a recombinogenic 3' end (not shown). (**E**) The newly synthesized strand that was originally stalled utilizes the HR machinery to form a D-loop allowing it to once again replicate off the original parental template, but now past the site of the previous stall-inducing lesion. (**F**) DNA replication now resumes off of the parental templates, generating a

double Holliday junction in its wake. (**C**) The double Holliday junction is efficiently resolved through the activities of the Sgs1 complex.

1. *Branzei, D., Vanoli, F. and Foiani, M. (2008) SUMOylation regulates Rad18-mediated template switch. Nature, 456, 915-920.*
2. *Liberi, G., Maffioletti, G., Lucca, C., Chiolo, I., Baryshnikova, A., Cotta-Ramusino, C., Lopes, M., Pellicioli, A., Haber, J.E. and Foiani, M. (2005) Rad51-dependent DNA structures accumulate at damaged replication forks in sgs1 mutants defective in the yeast ortholog of BLM RecQ helicase. Genes Dev, 19, 339-350.*
3. *Chavez, A., George, V., Agrawal, V., and Johnson, F. B. (2010) J Biol Chem* **285**, 11922-11930

Ω Adapted from:

Sun, W., Nandi, S., Osman, F., Ahn, J.S., Jakovleska, J., Lorenz, A. and Whitby, M.C. (2008) The FANCM ortholog Fml1 promotes recombination at stalled replication forks and limits crossing over during DNA double-strand break repair. Mol Cell, 32, 118-128.

Chavez, A., Tsou, A.M. and Johnson, F.B. (2009) Telomeres do the (un)twist: helicase actions at chromosome termini. Biochim Biophys Acta, 1792, 329-340.

Supplemental Figure 1

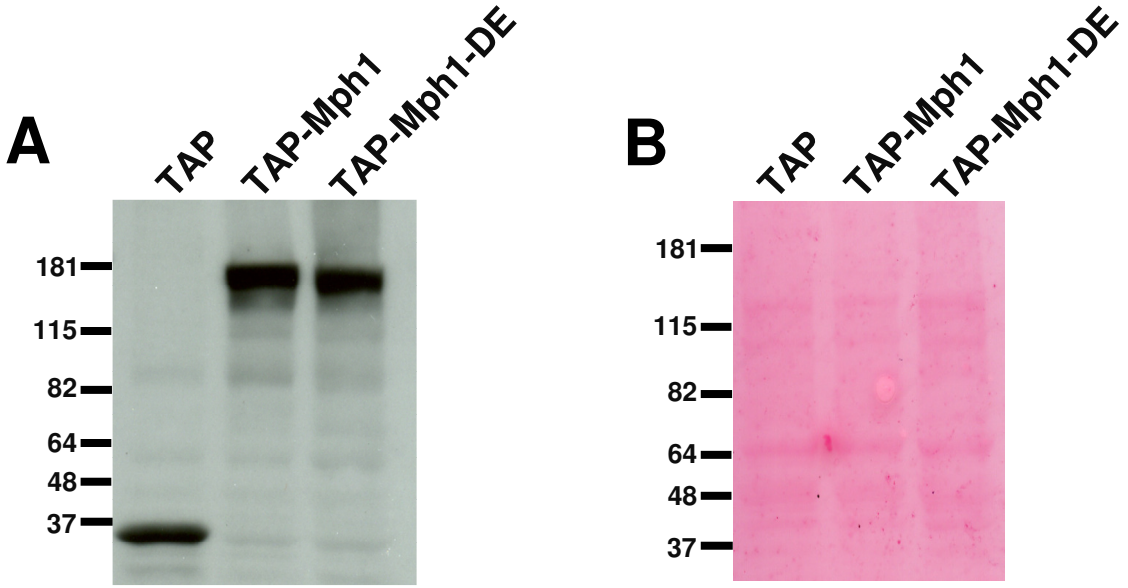

Supplemental Figure 2

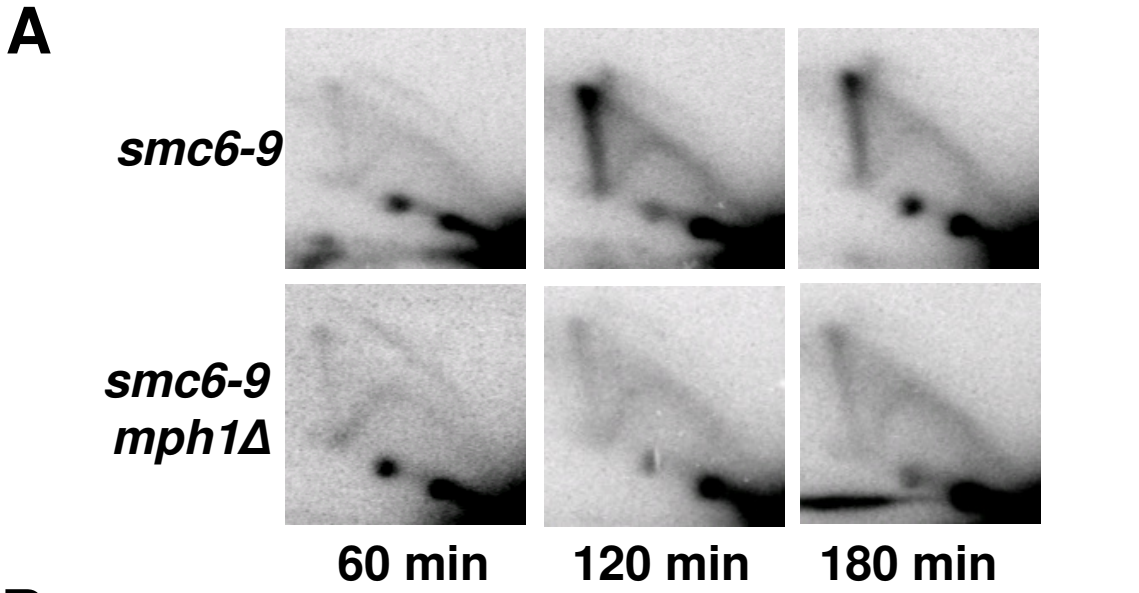

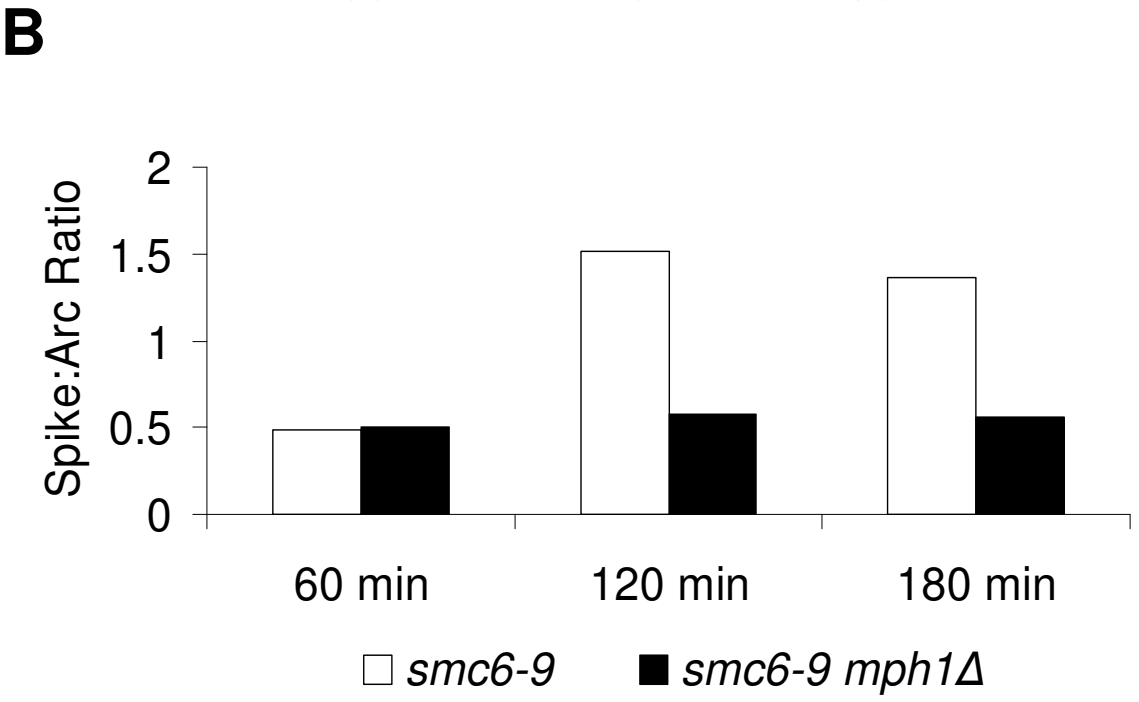

Supplemental Figure 3

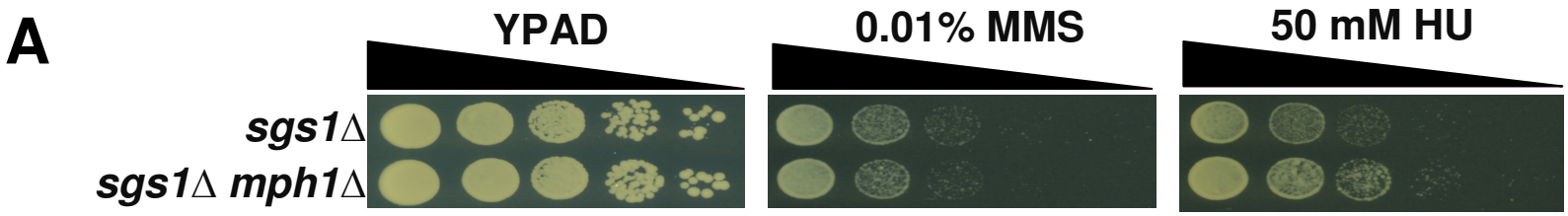

Supplemental Figure 4

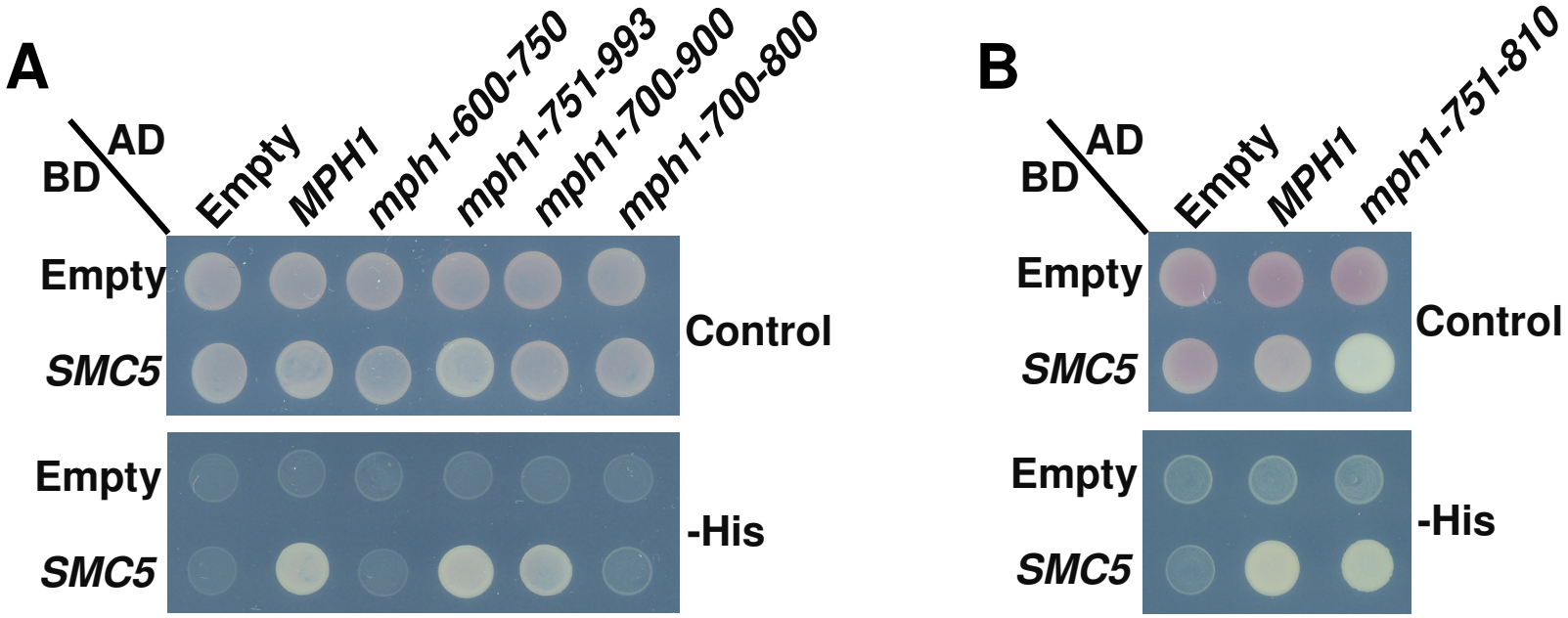

Supplemental Figure 5

A

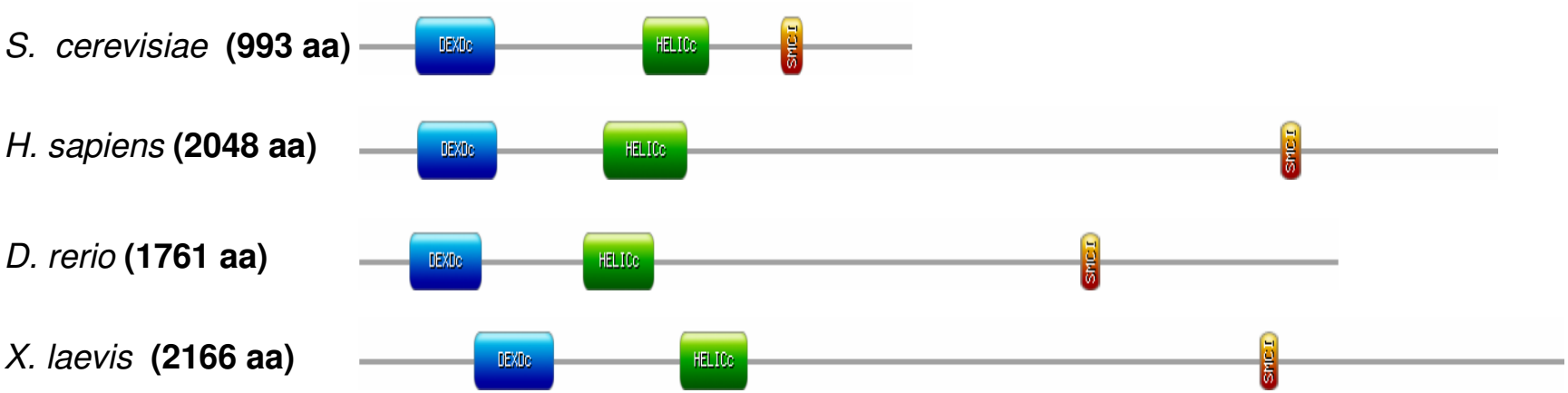

B

```
S. cerevisiae  NPSKKRKIFKALDNLENDSTEEASSSLETEDEEVSDDNN
H. sapiens     AHS-KKKLSRII--LPDDSSEENNVNDKRESNIAVNPST
D. rerio       HRSIKKF-PRGAARQFLD--EEAELS-EDEDGDVSSDED
X. laevis      LSSKKRKRSKQTARHFLD--EEAELSSEGA-EFVSSDEN
```

Supplemental Figure 6

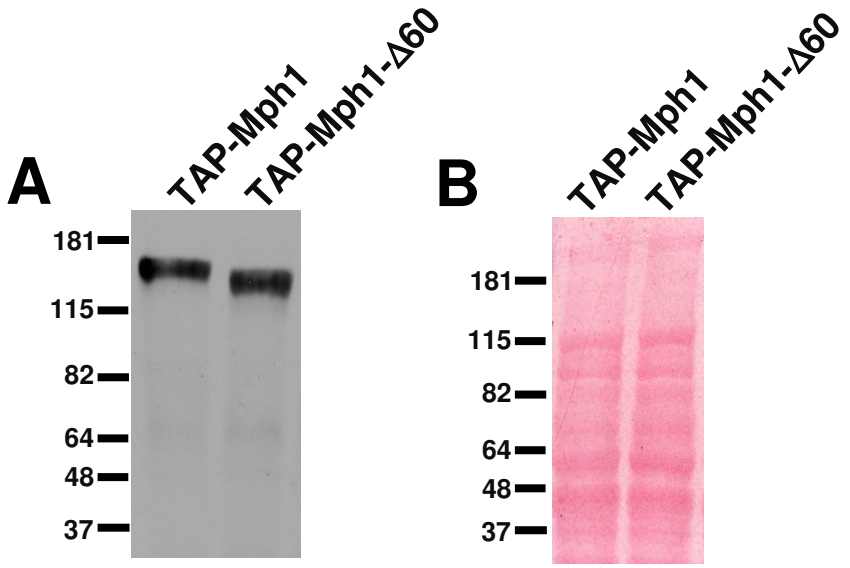

Supplemental Figure 7

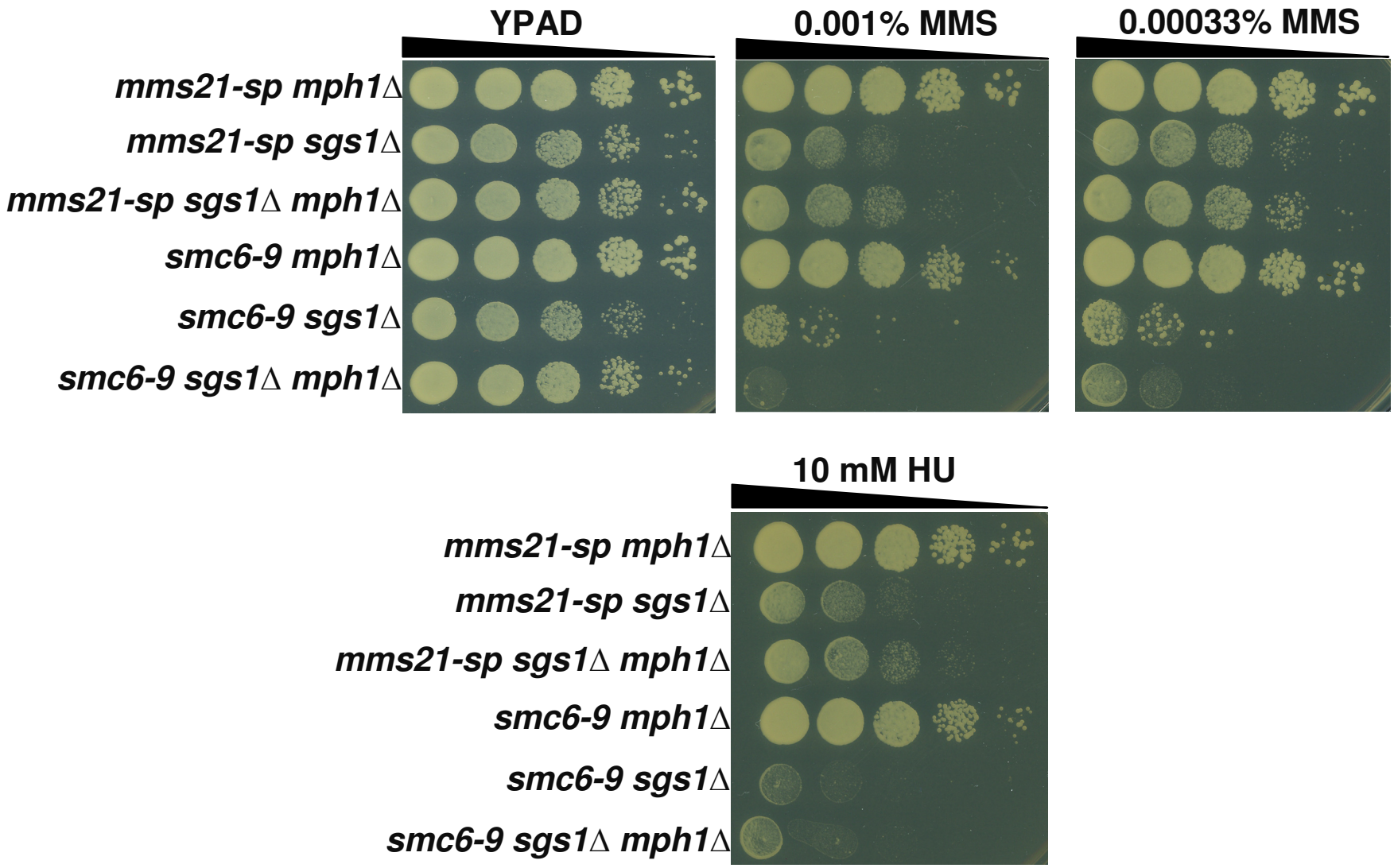

Supplemental Figure 8

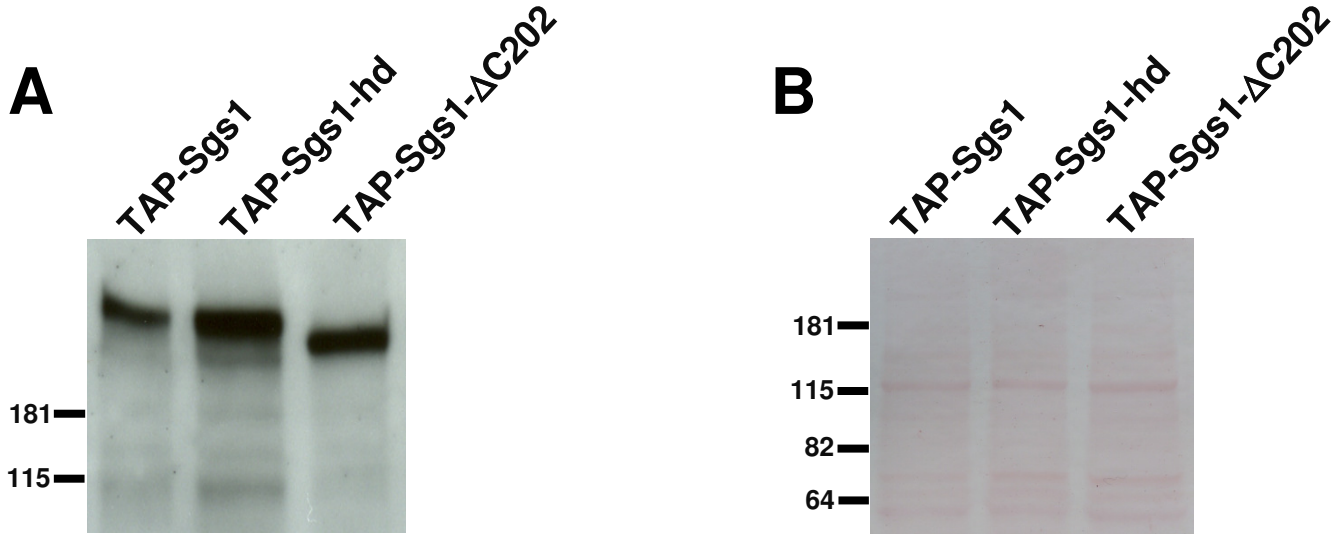

Supplemental Figure 9

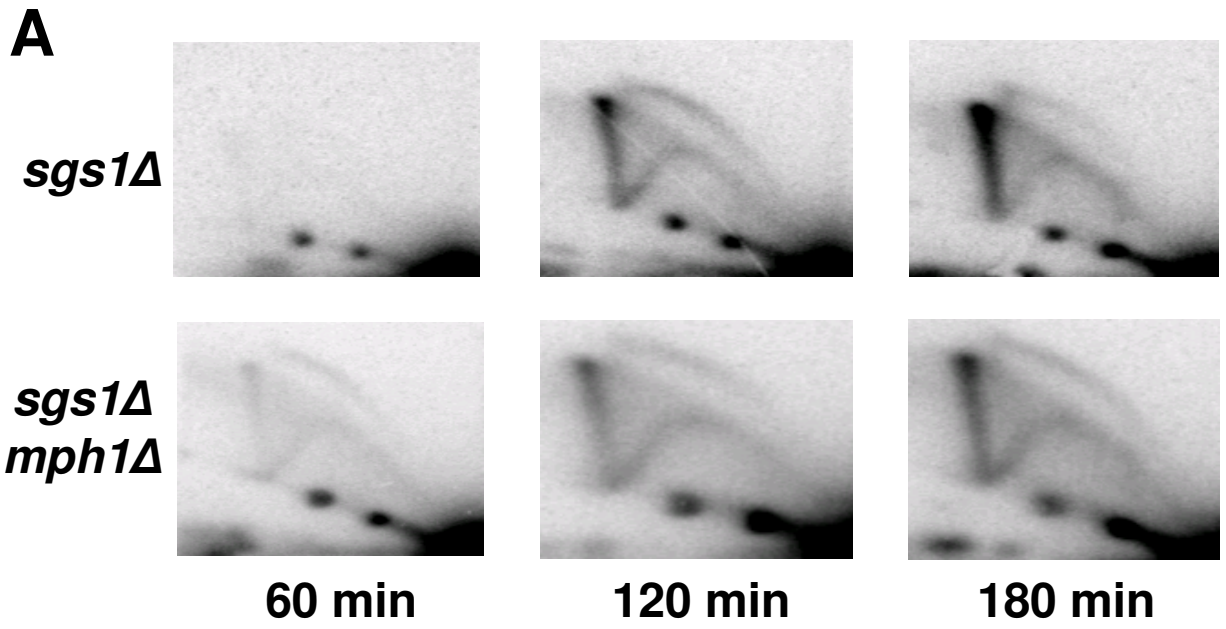

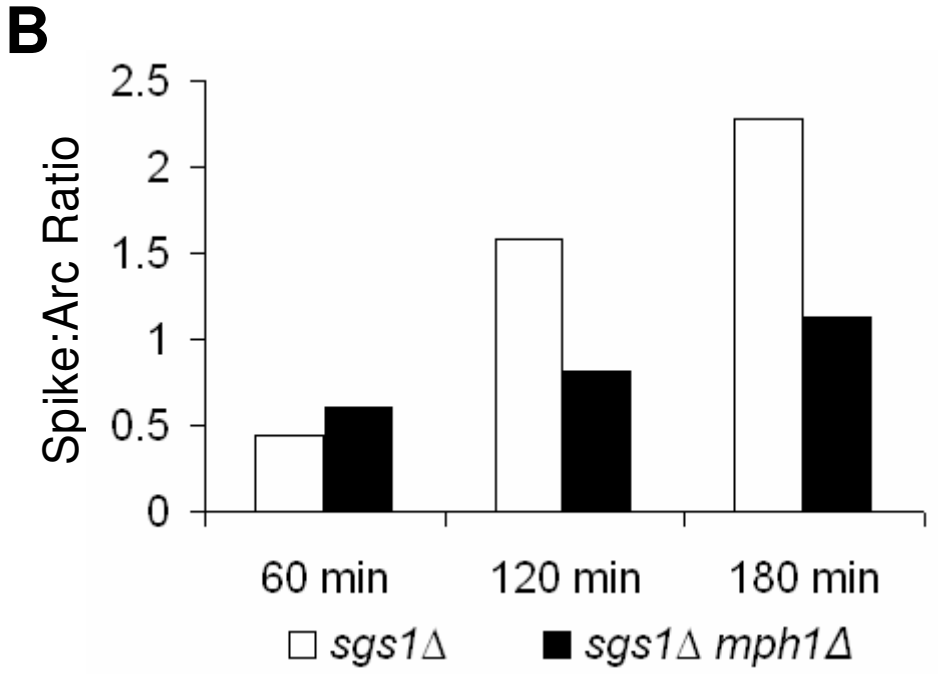

Supplemental Figure 10

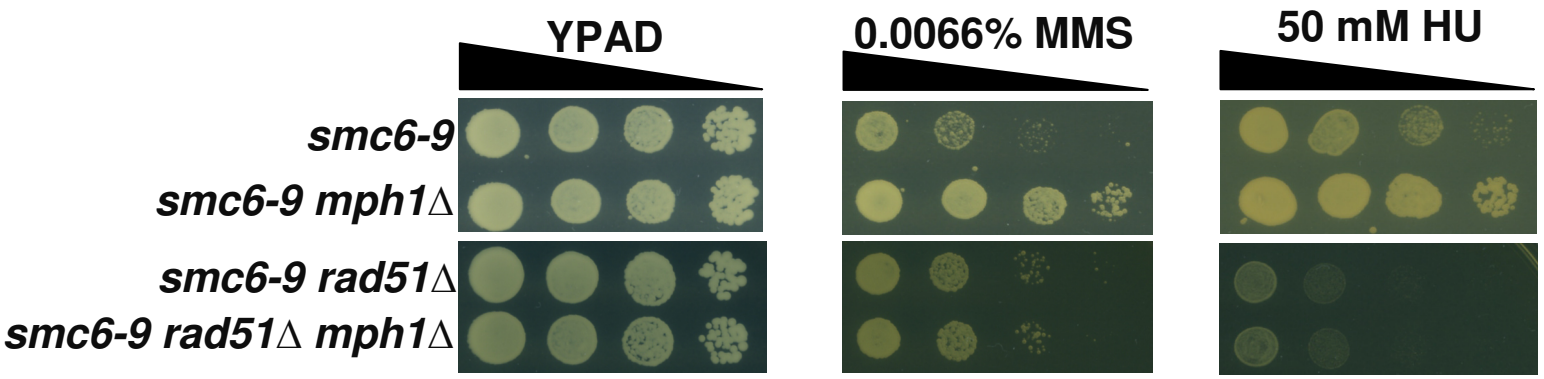

Supplemental Figure 11

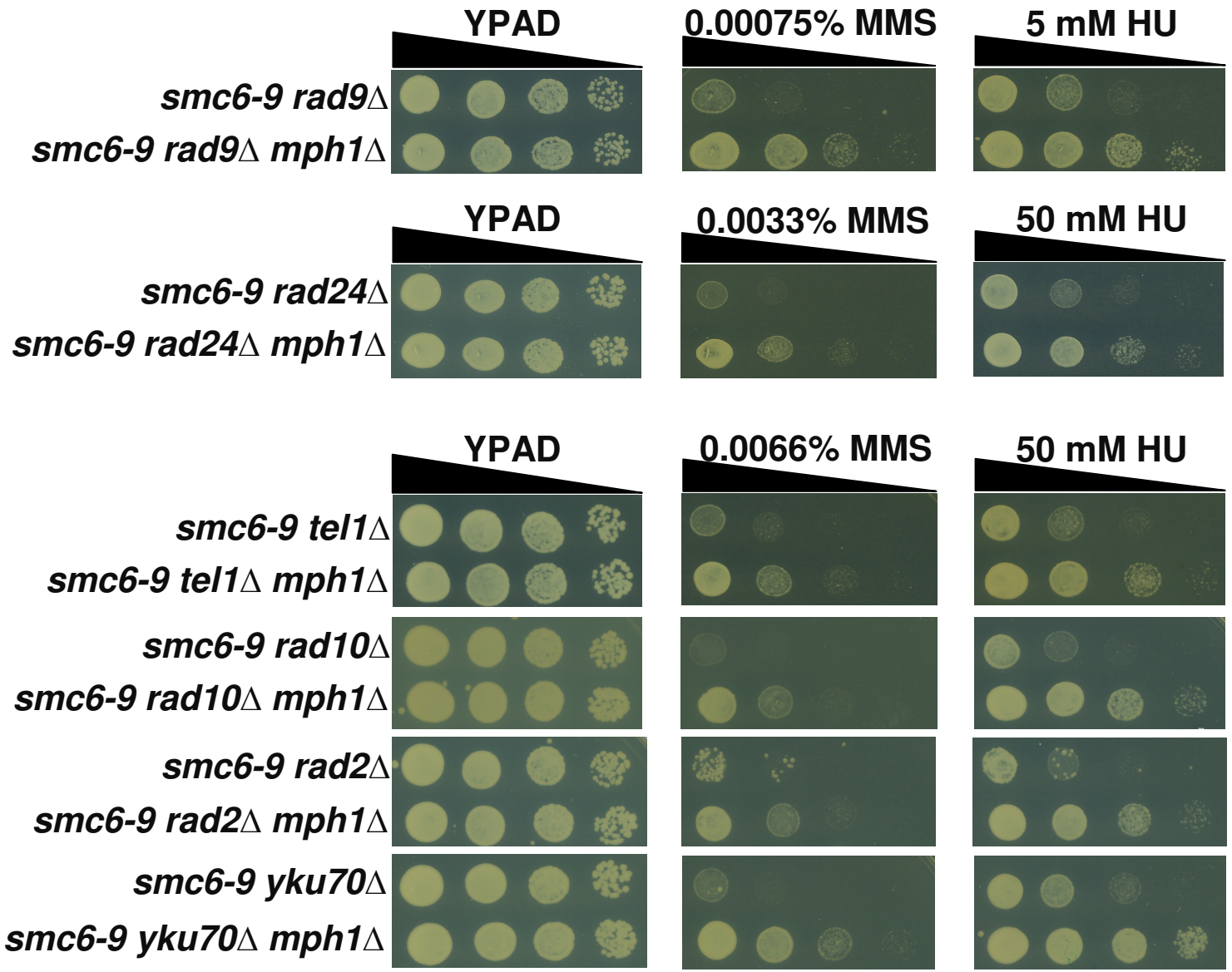

Supplemental Figure 12